

GROUP EXPECTATION POLICY OPTIMIZATION FOR HETEROGENEOUS REINFORCEMENT LEARNING

Han Zhang*, Ruibin Zheng, Zexuan Yi, Zhuo Zhang, Hanyang Peng, Hui Wang, Zike Yuan, Cai Ke, Shiwei Chen, Jiacheng Yang, Yangning Li, Xiang Li, Jiangyue Yan, Yaoqi Liu, Liwen Jing, Jiayin Qi, Ruifeng Xu, Binxing Fang, Yue Yu†

ABSTRACT

As single-center computing approaches power constraints, decentralized training becomes essential. However, traditional Reinforcement Learning (RL) methods, crucial for enhancing large model post-training, cannot adapt to decentralized distributed training due to the tight coupling between parameter learning and rollout sampling. For this, we propose **HeteroRL**, a heterogeneous RL architecture that decouples these processes, enabling stable training across geographically distributed nodes connected via the Internet. The core component is Group Expectation Policy Optimization (GEPO), an asynchronous RL algorithm robust to latency caused by network delays or heterogeneity in computational resources. Our study reveals that high latency significantly increases KL divergence, leading to higher variance in importance sampling weights and training instability. GEPO mitigates this by exponentially reducing the variance of importance weights through group expectation weight, achieving exponential variance reduction theoretically. Experiments show that GEPO achieves superior stability, with only a 3% performance drop from online to 1800s latency and up to $2.7\times$ the performance of GRPO under the most extreme conditions, demonstrating strong potential for decentralized RL in heterogeneous networks.

1 INTRODUCTION

In recent years, Large-scale Language Models (LLMs) (Dubey et al., 2024; Yang et al., 2025; Brown et al., 2020) have achieved remarkable progress through pre-training on massive text corpora. However, as high-quality pre-training data becomes increasingly scarce, the paradigm of solely relying on scaling up model size and data volume is encountering diminishing returns (Kaplan et al., 2020), with limited room for further performance improvement. To further unlock the potential of LLMs, particularly in enhancing their capabilities on complex tasks such as mathematical reasoning (Shao et al., 2024), Reinforcement Learning (RL) (Dai et al., 2024) has been widely adopted as an effective post-training method.

Despite the significant potential of RL in enhancing LLM reasoning, its large-scale distributed training faces serious systemic challenges. On the one hand, traditional synchronous RL frameworks require strict alternation between rollout generation and policy/critic updates (Noukhovitch et al., 2024; Ji et al., 2023; Gao et al., 2023; Warnell et al., 2018). This leads to significant idle time for computational resources (e.g., GPUs) while waiting for the completion of the longest sequences when processing long reasoning outputs, severely constraining training efficiency (Fu et al., 2025). On the other hand, with the explosive growth in model size and data requirements, the computational power of a single node is no longer sufficient. Leveraging geographically distributed heterogeneous computing resources to form computing networks for decentralized training has become an inevitable trend (Team et al., 2025). In this scenario, network latency between different nodes is inevitable, resulting in a temporal gap (i.e., latency) between the policy version used by the sampler and learner. Most existing RL frameworks are tightly coupled with homogeneous, low-latency computing

* Email: zhangh04@pcl.ac.cn.

† Yue Yu is Corresponding author.

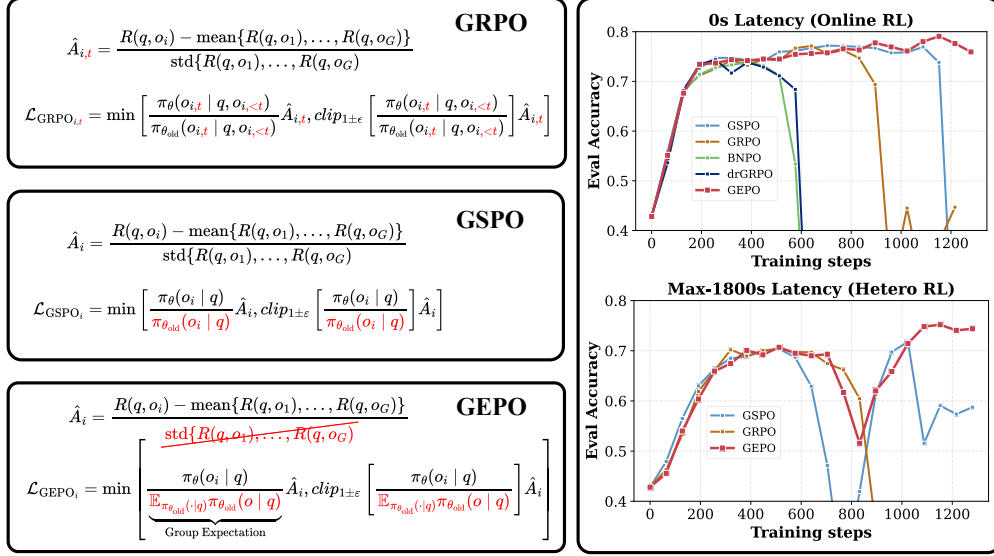


Figure 1: Left: GEPO improves upon GRPO and GSPO by employing group-level importance weights to enhance training stability. Right: In both zero-delay (online) and high-delay (up to 1800 seconds) heterogeneous reinforcement learning scenarios, GEPO demonstrates superior stability and better evaluation performance.

environments and struggle to effectively address the challenges posed by such heterogeneity and latency, limiting their applicability in more general scenarios involving collaborative training across geographically distributed computing nodes connected via the Internet.

To address the above challenges, we propose HeteroRL (Heterogeneous Reinforcement Learning), a reinforcement learning framework specifically designed for asynchronous and heterogeneous environments, aiming to achieve efficient and robust mathematical reasoning training for large language models. The core idea of HeteroRL is to decouple the two computationally intensive yet distinct tasks in the RL pipeline—rollout sampling and parameter learning—and deploy them on independent computing nodes that may have different computational capabilities. The sampler is responsible for continuously generating reasoning trajectories, while the learner asynchronously updates the model parameters based on the collected trajectory data. Both processes run continuously without waiting for each other, communicating via dedicated networks or the internet to transfer model parameters and rollout data at low frequencies or under high latency. The heterogeneous reinforcement learning scenario differs from the traditional online or offline reinforcement learning scenario.

Due to differences in computational efficiency across heterogeneous hardware and network conditions between geographically distributed nodes, there is an inevitable delay between training and sampling (mutual transmission). Our experiments show that excessive latency severely inflates KL divergence, disrupting importance sampling by significantly increasing the variance of importance weights, which in turn degrades training stability and limits the achievable performance ceiling.

In summary, our key contributions are as follows:

Framework: We propose HeteroRL, an asynchronous reinforcement learning framework designed for heterogeneous compute networks, enabling decentralized training of large language models (LLMs) on mathematical reasoning tasks.

Insight: We identify a strong correlation between latency and the KL divergence between the rollout sampler and the learner. High latency induces excessive divergence, leading to training instability and collapse.

Algorithm: We introduce Group Expectation Policy Optimization (GEPO), which improves upon the importance sampling mechanism in GRPO (Shao et al., 2024). We theoretically show that GEPO exponentially reduces the variance of importance weights, and empirically demonstrate its superior stability and efficiency — not only under high-latency conditions, but also in the ideal zero-latency setting.

Evaluation: Experiments on mathematical reasoning benchmarks show that HeteroRL outperforms RL baselines in both performance and stability, under both synchronous and asynchronous settings.

This work provides both algorithmic and system-level advancements for scalable LLM post-training, and establishes a practical foundation for large-scale distributed AI training in future heterogeneous compute network environments.

2 BACKGROUND

2.1 PROBLEM DEFINITION AND NOTATION

Consider a standard policy gradient framework. Let π_θ denote the language model policy (i.e., the Actor) parameterized by θ , x be an input prompt (e.g., a math problem), and $y = (y_1, \dots, y_T)$ be the output sequence generated by the model (e.g., a chain-of-thought solution). The environment provides a scalar reward $r(y)$ based on the outcome of y (e.g., whether the final answer is correct). We define the following core notation:

- π_{θ_k} (short for q): the policy used by the *sampler* at time step k to generate rollout trajectories.
- $\pi_{\theta_{k+\tau}}$ (short for p): the latest policy at the *learner* at time step $k + \tau$, used for gradient updates.
- τ : *policy staleness*, representing the discrepancy in policy versions between the sampler and the learner, caused by network transmission delays and computational asynchrony. In our setting, τ is a random variable rather than a fixed constant.
- y : a trajectory sampled from the stale policy π_{θ_k} .
- $r(x, y)$: the reward for response y given input x .
- $A(x, y)$: the advantage for response y to input x , typically defined as $A(x, y) = r(x, y) - b(x)$, where $b(x)$ is a baseline reward computed for input x . In this paper, we use the within-group average reward (Shao et al., 2024) as the baseline $b(x) = \frac{1}{G} \sum_{j=1}^G r(x, y_j)$.

The goal of RL is to optimize the policy π_θ to maximize the expected cumulative reward. To reduce gradient variance, an advantage function $A(y)$ is used, leading to the objective:

$$\mathcal{L}(\theta) = \mathbb{E}_{y \sim \pi_\theta(\cdot|x)} \left[A(y) \sum_{t=1}^T \nabla_\theta \log \pi_\theta(y_t|x) \right]. \quad (1)$$

3 GEPO: GROUP EXPECTATION POLICY OPTIMIZATION

Our method builds upon the group-based policy optimization paradigm of GRPO and introduces the Group Expectation Importance Sampling mechanism. We emphasize a paradigm shift from *token-level* to *group-level* importance weighting, which significantly reduces the variance of importance weights and alleviates gradient instability during training.

3.1 GROUP EXPECTATION IMPORTANCE WEIGHTING

To enhance the stability of importance weights, we propose the **Group Expectation Importance Weight** (GEIW) mechanism, which replaces the individual proposal probability $q(y|x)$ in the standard importance weight $\frac{p(y|x)}{q(y|x)}$ with its group-wise expected value

under the current prompt x , denoted as $\widehat{\mathbb{E}}_q[q(y|x)]$. Inspired by GRPO, for each input x , we generate a group of G responses $\{y_1, \dots, y_G\} \sim q(\cdot|x)$ to form a sampling group. Since G is typically much smaller than the full policy space and top- P /top- K sampling leads to $\sum_{i=1}^G q(y_i|x) \gg 1$, the vector $(q(y_1|x), \dots, q(y_G|x))$ does not constitute a valid probability distribution. Simply using the arithmetic mean $\frac{1}{G} \sum_{i=1}^G q(y_i|x)$ would introduce bias due to ignoring the relative sampling probabilities. To obtain a more accurate estimate, we employ a weighted expectation:

$$\widehat{\mathbb{E}}_q[q(y|x)] \approx \sum_{i=1}^G \widehat{q(y_i|x)} \cdot q(y_i|x) = \frac{\sum_{i=1}^G q(y_i|x)^2}{\sum_{i=1}^G q(y_i|x)}, \quad (2)$$

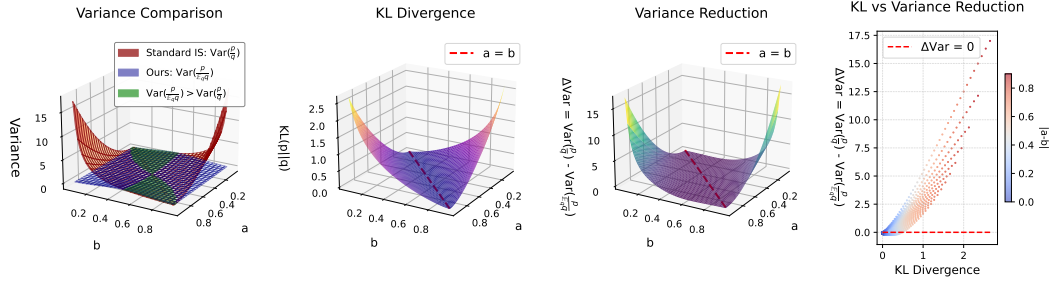
where $\widehat{q(y_i|x)} = \frac{q(y_i|x)}{\sum_{j=1}^G q(y_j|x)}$ is the within-group normalized probability, serving as an empirical estimate of the sampling likelihood of each y_i . We define the GEIW importance weight as:

$$w_{\text{GEIW}}(y|x) = \frac{p(y|x)}{\widehat{\mathbb{E}}_q[q(y|x)]}. \quad (3)$$

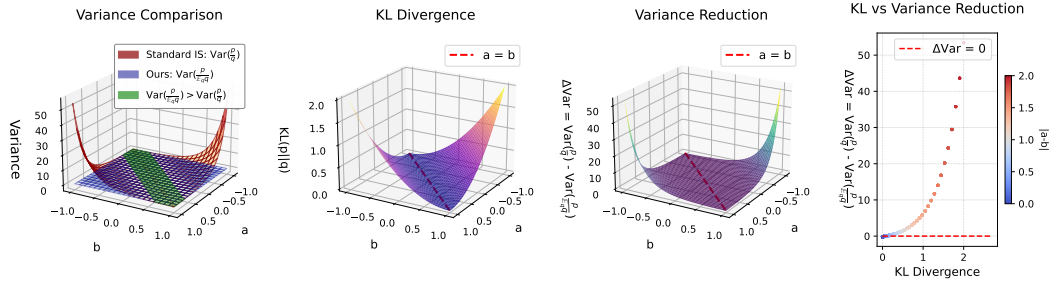
The key advantages of this mechanism are as follows:

Numerically stable and gradient-effective: The denominator is decoupled from any single $q(y|x)$, avoiding extreme weight values when individual proposal probabilities approach zero. Although $\text{clip}(1 \pm \epsilon)$ can also improve numerical stability, the gradients of the clipped tensors will be set to zero, effectively skipping this data point (ineffective gradient).

Biased yet low-variance: By leveraging within-group statistical information, GEIW provides a more reliable scale estimate. Even under large divergence between p and q , $\widehat{\mathbb{E}}_q[q(y|x)]$ remains well-conditioned, effectively preventing gradient explosion. Although this estimator introduces a small bias (w_{GEIW} is a biased estimator), both theoretical analysis (see Theorem 1) and empirical results demonstrate that it significantly reduces variance under high KL divergence, yielding more stable gradient directions and improved training convergence.



(a) Variance comparison of $\frac{p}{q}$ and $\frac{p}{\widehat{\mathbb{E}}_q[q]}$ under Bernoulli distributions, where $p \sim \text{Bernoulli}(a)$ and $q \sim \text{Bernoulli}(b)$.



(b) Variance comparison of $\frac{p}{q}$ and $\frac{p}{\widehat{\mathbb{E}}_q[q]}$ under Gaussian distributions, where $p \sim \mathcal{N}(a, 1)$ and $q \sim \mathcal{N}(b, 1)$.

Figure 2: In high-KL regions, $\text{Var}[\frac{p(y|x)}{\widehat{\mathbb{E}}_q[q(y|x)]}] \ll \text{Var}[\frac{p(y|x)}{q(y|x)}]$.

Theorem 1. Let p, q be discrete probability distributions. Then there exists a constant C such that:

$$\text{Var} \left[\frac{p(y|x)}{q(y|x)} \right] - \text{Var} \left[\frac{p(y|x)}{\mathbb{E}_q[q(y|x)]} \right] \geq \exp(D_{\text{KL}}(p||q)) - C. \quad (4)$$

In particular, when $D_{\text{KL}}(p||q) > \log C$, it holds that $\text{Var} \left[\frac{p(y|x)}{q(y|x)} \right] > \text{Var} \left[\frac{p(y|x)}{\mathbb{E}_q[q(y|x)]} \right]$.

Theorem 1 shows that GEPO can **exponentially reduce the variance of importance weights**, making it particularly well-suited for heterogeneous RL training under high KL divergence. The full mathematical proof is provided in Appendix A. As shown in Figure 2, we visualize the relationship between KL divergence and importance weight variance when both p and q are Bernoulli or Gaussian distributions with varying parameters. The results indicate that in the high-KL regime, the group expectation approach significantly reduces the variance of importance weights, which benefits training stability under high network latency. Nevertheless, there exist regimes—such as the green regions in the plots—where our method incurs a slight increase in variance.

The difference across all GRPO-like algorithms lies in the computation of the importance weights, as detailed in Listing 1:

```

1 if self.loss_type in ["grpo", "dr_grpo", "bnpo"]: # Token level
2     coef_1 = learner_token_p / sampler_token_p
3 elif self.loss_type == "gspe": # Sequence level
4     coef_1 = learner_seq_p / sampler_seq_p
5 elif self.loss_type == "gepo": # Group level
6     normalized_q = sampler_seq_p.detach() / (sampler_seq_p.sum().
7         detach())
8     coef_1 = learner_seq_p / (normalized_q * sampler_seq_p).sum()

```

Listing 1: Coefficient computation for different policy optimization methods

3.2 GRADIENT COMPARISON ACROSS TOKENS

What does the GEPO update do? For a mechanistic understanding of GEPO, it is useful to analyze the gradient of the loss function $\mathcal{L}_{\text{GEPO}}$. The equivalent gradient of each token in a group with respect to the parameters θ of GRPO, GSPO and GEPO can be written as:

$$\frac{\partial \mathcal{L}(\theta)}{\partial \theta} = \mathbf{A} \odot \underbrace{\begin{bmatrix} \frac{p'_{1,1}(\theta)}{q_{1,1}} & \dots & \frac{p'_{1,T}(\theta)}{q_{1,T}} \\ \vdots & \ddots & \vdots \\ \frac{p'_{G,1}(\theta)}{q_{G,1}} & \dots & \frac{p'_{G,T}(\theta)}{q_{G,T}} \end{bmatrix}}_{\text{GRPO}} \quad \text{or} \quad \underbrace{\begin{bmatrix} \frac{p'_{1,1}(\theta)}{q_1} & \dots & \frac{p'_{1,T}(\theta)}{q_1} \\ \vdots & \ddots & \vdots \\ \frac{p'_{G,1}(\theta)}{q_G} & \dots & \frac{p'_{G,T}(\theta)}{q_G} \end{bmatrix}}_{\text{GSPO}} \quad \text{or} \quad \underbrace{\begin{bmatrix} \frac{p'_{1,1}(\theta)}{\mathbb{E}_q q} & \dots & \frac{p'_{1,T}(\theta)}{\mathbb{E}_q q} \\ \vdots & \ddots & \vdots \\ \frac{p'_{G,1}(\theta)}{\mathbb{E}_q q} & \dots & \frac{p'_{G,T}(\theta)}{\mathbb{E}_q q} \end{bmatrix}}_{\text{GEPO (ours)}}, \quad (5)$$

where $\mathbf{A} \in \mathbb{R}^{G \times T}$ is token-level advantages matrix, \odot denotes Hadamard product, $q_{i,t} = q(y_t^i | x^i, y_{<t}^i)$, $q_i = q(y^i | x^i)$, and $\mathbb{E}_q q = \mathbb{E}_q[q(y|x)]$. From the perspective of gradient stability, GSPO unifies the coefficient of the gradient for each token within a sequence to $\frac{1}{q(y^i|x^i)}$ ($i = 1, 2, \dots, G$). In contrast, GEPO sets the denominator for the gradient of each token within a group to $\frac{1}{\mathbb{E}_q q}$. Experimental results demonstrate that this approach effectively stabilizes the gradients across a group during the training process. Notably, GRPO uses token-level coefficients, GSPO uses sequence-level coefficients, and GEPO uses group-level coefficients. Empirical results show that coarser coefficient granularity leads to greater training stability. This indicates that leveraging 'high-level' statistical information, such as group expectations, improves robustness and reduces variance, enhancing the overall stability of the reinforcement learning process.

4 EXPERIMENTS

4.1 EXPERIMENTAL SETUP

Model, Dataset and Benchmarks We conduct reinforcement learning training and evaluation on the Qwen3-1.7B model. The model is trained by strong-to-weak distillation (Yang et al., 2025), but has not been tuned with any RL. We use 8290 MATH lv.3-5 samples as the training set, 200 MATH lv.3-5 samples as the evaluation set, reporting average Pass@1 over 8 sampled responses on MATH500, AMC23, AIME24, and AIME25 benchmarks. We compare our method against baseline methods GRPO (Shao et al., 2024), GSPO (Zheng et al., 2025), BNPO (Xiao et al., 2025), and Dr.GRPO (Liu et al., 2025) under both homogeneous and heterogeneous computing settings.

Heterogeneous Computing Environment As shown in Figure 3, we perform heterogeneous training across five compute nodes: one learner node and four sampler nodes, forming a star-shaped topology centered at the learner. During training, the sampler nodes generate rollout data, which is transmitted over the network to the learner node in a streaming fashion. The learner updates the model parameters and periodically broadcasts the updated weights back to the sampler nodes. The learner processes incoming rollouts in the order they arrive, operating within a fixed time window for data eligibility. Since data is transmitted in batch units—each containing text, generation probabilities, and rewards—a maximum delay of 1800 seconds is sufficient for typical network conditions. Within this window, the iteration gap (in terms of gradient updates) between the learner and samplers remains within 64 steps.

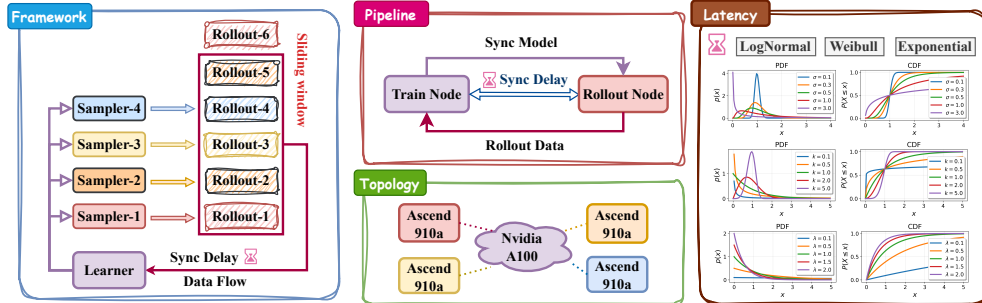


Figure 3: The Overview of HeteroRL. By decoupling sampling and training, HeteroRL enables decentralized distributed RL training of LLMs across five compute nodes: one parameter update node (learner) and four data generation nodes (sampler), forming a star-shaped network topology. Network delays between the sampler and learner nodes are explicitly modeled and can be simulated using stochastic distributions such as the log-normal or Weibull distribution.

4.2 MAIN EXPERIMENTAL RESULTS

As shown in Table 1, for the Qwen3-1.7B backbone model, GEPO achieved the highest average performance among all policy optimization methods, demonstrating its effectiveness. It is worth noting that GRPO experienced a sharp performance drop in the third epoch of training. While GSPO could somewhat delay this performance collapse, it still could not avoid the eventual degradation. In contrast, GEPO perfectly suppressed the occurrence of such collapses, exhibiting only minor fluctuations.

From the experimental results in Table 1, it can be observed that GEPO outperforms existing state-of-the-art methods in both optimal performance and final performance, regardless of whether in zero-delay or high-delay scenarios. During the training process of GRPO and GSPO, after reaching a performance peak, they are prone to training collapse, resulting in a significant gap between their final performance and best performance. Figure 4 records one set of training processes. From the training curves, it can be seen that GEPO is more stable

Table 1: Performance comparison using Qwen3-1.7B (thinking mode).

Method	AMC23		AIME2024		AIME2025		MATH500		Average	
	Best	Last	Best	Last	Best	Last	Best	Last	Best	Last
Qwen3-1.7B	25.6	-	1.6	-	3.9	-	54.7	-	21.5	-
Max Tolerable Delay 0										
BNPO	54.3	0.0	18.4	0.0	19.1	0.0	78.7	0.0	42.6	0.0
Dr.GRPO	53.4	14.3	19.1	1.6	18.8	2.0	78.6	35.9	42.5	13.5
GRPO	56.3	23.4	20.7	0.4	19.9	2.3	79.8	49.7	44.2	19.0
GSPO	54.1	27.8	23.8	3.1	20.7	4.3	79.9	62.1	44.6	24.3
GEPO (ours)	56.9	56.9	21.9	16.4	20.3	14.1	80.4	78.1	44.9	41.4
Max Tolerable Delay 64										
BNPO	45.0	43.1	12.1	11.3	12.5	10.1	71.1	69.3	35.2	33.5
Dr.GRPO	48.4	48.4	17.2	17.2	14.8	14.8	73.9	73.9	38.6	38.6
GRPO	46.6	46.6	19.1	14.5	14.8	14.8	74.9	74.9	38.9	37.7
GSPO	54.4	23.8	17.6	1.6	17.6	2.7	78.2	55.6	41.9	20.9
GEPO (ours)	53.8	53.8	21.9	21.9	18.8	18.8	79.6	79.6	43.5	43.5

compared to GRPO and GSPO, with consistently lower variance of importance weights and no significant changes in gradient norms, thus the reward value shows no obvious decline at the end of training. In this experiment, we used identical hyperparameters (such as a KL penalty of 0.005 to maintain training stability) and the same random seed to ensure rollout data consistency as much as possible. None of the methods employed defensive sampling mechanisms.

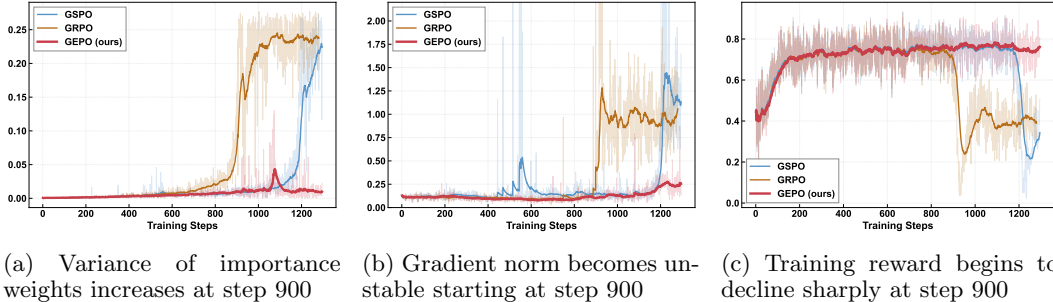


Figure 4: Synchronous changes in importance sampling variance, training gradient norm, and training reward. Compared to GRPO and GSPO, our proposed GEPO maintains more stable importance weight variance, resulting in less drastic gradient changes, more stable training, and no decline in training reward.

4.3 ANALYSIS STUDIES

Impact of Latency As shown in Figure 5, we analyze the changes in KL divergence between the trainer and sampler, variance of importance weights, and estimation error of the expected value of the advantage function (optimization objective) during heterogeneous RL training as latency increases. We observe that latency leads to increased KL divergence (Figure 9a), which in turn causes an increase in the variance of importance weights (Figure 9b), ultimately resulting in increased estimation error of the expected advantage function (Figure 9c). Since the optimization objective is to maximize the estimated expectation of the advantage function, large estimation errors will cause significant fluctuations in gradients, thereby affecting training stability and performance.

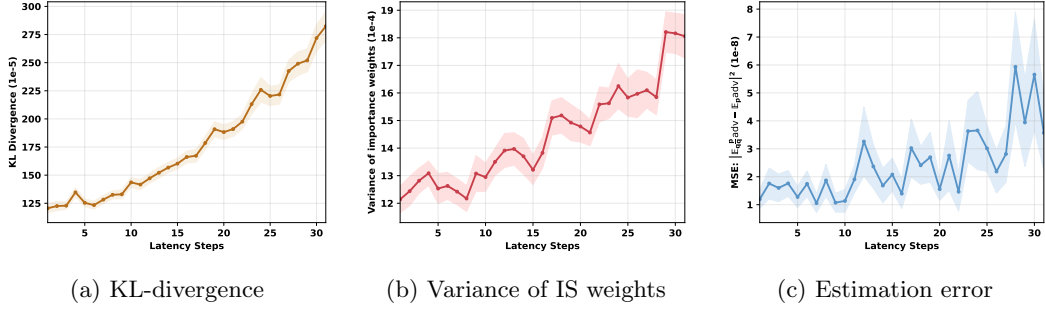


Figure 5: Trends of latency and importance sampling variance

Correlation Analysis Figure 6 further analyzes the correlation between training delay steps, importance sampling variance, and estimation error of the expected advantage function. We find that the correlation coefficients among these three variables range from 0.76 to 0.96 ($\alpha = 0.05$), indicating that higher latency leads to greater training instability. However, we observe that changes in KL divergence are not solely related to latency but also depend on the model and sampled data. While higher latency increases the probability of KL divergence spikes, it does not always lead to training collapse.

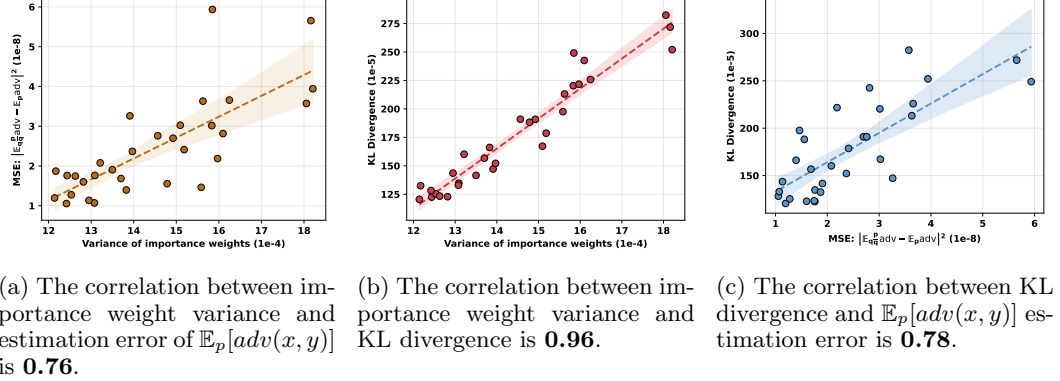


Figure 6: Correlation analysis (95% CI) of training delay steps, importance sampling variance, and estimation error of expected advantage function

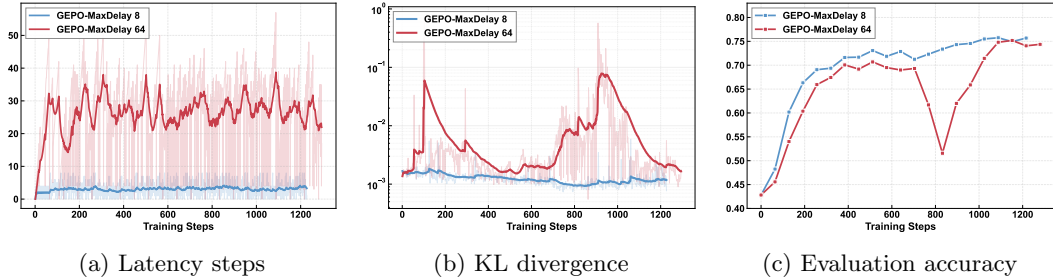


Figure 7: Training processes under different latency conditions

Challenges of High Latency To demonstrate that high latency reduces training stability, we compared training processes with maximum delays of 8 steps and 64 steps respectively. As shown in Figure 7, under the maximum delay of 64 steps, particularly when the delay reaches its peak (around step 900), the KL divergence increases rapidly and the evaluation accuracy significantly decreases. This experiment confirms our hypothesis that latency

increases instability. Although GEPO significantly improves training stability compared to methods like GRPO, it is still affected by latency-induced issues (performance drop around step 900), indicating that heterogeneous reinforcement learning in high-latency scenarios remains a challenging research direction. Better methods should be able to mitigate the negative impact of latency on training, making the training process more stable.

5 RELATED WORK

In recent years, reinforcement learning (RL) has become central to post-training large language models (LLMs) Ziegler et al. (2019). Researchers have identified efficiency bottlenecks in traditional synchronous RL frameworks. Wu et al. (2025) first theoretically explored asynchronous RLHF (Ouyang et al., 2022), proposing to decouple generation and learning for ‘on-policy yet off-policy’ training. They found that algorithms like Online DPO Calandriello et al. (2024) are robust to policy mismatch, and larger models are more resilient—justifying asynchronous training at scale. Wu et al. introduced LlamaRL Wu et al. (2025), a distributed, asynchronous RL framework that decouples generation and optimization to reduce GPU idle time and improve resource utilization. However, it focuses on single-machine or small clusters, neglecting dynamic network delays in heterogeneous environments. To address practical efficiency, AREAL Fu et al. (2025) fully decouples generation and training, using staleness thresholds and a decoupled PPO objective (Schulman et al., 2017b) to handle outdated samples. It improves both training speed and final performance on reasoning and code tasks—but assumes stable networks, unlike the unpredictable, high-latency settings targeted by *HeteroRL*. *Prime Intellect* Team et al. (2025) offers a decentralized, asynchronous framework for community compute, ensuring trust via verifiable inference, stability via two-sided GRPO clipping, and controllable reasoning with length-aware rewards. These works motivate our design: a robust, delay-tolerant framework for heterogeneous, geographically distributed RLHF.

6 CONCLUSION

We present HeteroRL, an asynchronous reinforcement learning framework for training LLMs across geographically distributed, heterogeneous compute nodes, and introduce GEPO (Group Expectation Policy Optimization), a novel algorithm designed to stabilize training under high network latency. By decoupling rollout sampling from policy updates, HeteroRL eliminates synchronization bottlenecks. GEPO addresses the critical issue of exploding importance sampling variance caused by policy staleness, leveraging group-level expectation smoothing to exponentially reduce gradient variance—particularly under large KL divergence, as proven theoretically. Empirical results on mathematical reasoning benchmarks demonstrate that GEPO maintains training stability even under extreme 1800-second delays, with performance degradation limited to under 3% compared to synchronous training. It consistently outperforms GRPO, GSPO, and other baselines in both final accuracy and training robustness. This work establishes a scalable, delay-tolerant foundation for decentralized RLHF, enabling efficient LLM post-training in real-world heterogeneous networks.

AUTHOR CONTRIBUTIONS

The division of labor within the research team is as follows: **Han Zhang** was responsible for the design of the GEPO algorithm, preliminary implementation of the HeteroRL training framework, and technical report writing. **Ruibin Zheng** focused on optimizing the implementation of the HeteroRL training framework, improving data transmission execution logic in simulated latency scenarios, tuning model hyperparameters and prompts, creating visualizations, conducting model performance evaluations and participating in algorithm analysis. **Zexuan Yi** was responsible for implementing data transmission in real network environments and engineering the model synchronization mechanism. **Zhuo Zhang** contributed to experimental analysis and experimental design.

The defensive sampling mechanism was initially proposed by the **Qwen3-235B-A22B-2507 model**. While our experiments demonstrated that this mechanism can enhance training stability, we note that no existing literature has formally documented or proposed such a defensive sampling mechanism.

ACKNOWLEDGMENTS

This work is supported by the Major Key Project of PCL (Grant No. PCL2025AS209). We thank **Xiang Li** for verifying the theoretical proofs in this paper, and **Wei Li** for providing technical support on hardware infrastructure and system maintenance.

REFERENCES

- Tom Brown, Benjamin Mann, Nick Ryder, Melanie Subbiah, Jared D Kaplan, Prafulla Dhariwal, Arvind Neelakantan, Pranav Shyam, Girish Sastry, Amanda Askell, Sandhini Agarwal, Ariel Herbert-Voss, Gretchen Krueger, Tom Henighan, Rewon Child, Aditya Ramesh, Daniel Ziegler, Jeffrey Wu, Clemens Winter, Chris Hesse, Mark Chen, Eric Sigler, Mateusz Litwin, Scott Gray, Benjamin Chess, Jack Clark, Christopher Berner, Sam McCandlish, Alec Radford, Ilya Sutskever, and Dario Amodei. Language models are few-shot learners. In *Proceedings of the International Conference on Neural Information Processing Systems*, pp. 1877–1901, 2020.
- Daniele Calandriello, Daniel Guo, Remi Munos, Mark Rowland, Yunhao Tang, Bernardo Avila Pires, Pierre Harvey Richemond, Charline Le Lan, Michal Valko, Tianqi Liu, et al. Human alignment of large language models through online preference optimisation. *arXiv preprint arXiv:2403.08635*, 2024.
- Josef Dai, Xuehai Pan, Ruiyang Sun, Jiaming Ji, Xinbo Xu, Mickel Liu, Yizhou Wang, and Yaodong Yang. Safe RLHF: Safe reinforcement learning from human feedback. In *Proceedings of the Twelfth International Conference on Learning Representations*, 2024.
- Abhimanyu Dubey, Abhinav Jauhri, Abhinav Pandey, Abhishek Kadian, Ahmad Al-Dahle, Aiesha Letman, Akhil Mathur, Alan Schelten, Amy Yang, Angela Fan, et al. The llama 3 herd of models. *ArXiv Preprint ArXiv:2407.21783*, 2024.
- Wei Fu, Jiaxuan Gao, Xujie Shen, Chen Zhu, Zhiyu Mei, Chuyi He, Shusheng Xu, Guo Wei, Jun Mei, Jiashu Wang, et al. Areal: A large-scale asynchronous reinforcement learning system for language reasoning. *arXiv preprint arXiv:2505.24298*, 2025.
- Leo Gao, John Schulman, and Jacob Hilton. Scaling laws for reward model overoptimization. In *Proceedings of the 40th International Conference on Machine Learning*, pp. 10835–10866, 2023.
- Jiaming Ji, Tianyi Qiu, Boyuan Chen, Borong Zhang, Hantao Lou, Kaile Wang, Yawen Duan, Zhonghao He, Jiayi Zhou, Zhaowei Zhang, et al. Ai alignment: A comprehensive survey. *ArXiv Preprint ArXiv:2310.19852*, 2023.
- Jared Kaplan, Sam McCandlish, Tom Henighan, Tom B Brown, Benjamin Chess, Rewon Child, Scott Gray, Alec Radford, Jeffrey Wu, and Dario Amodei. Scaling laws for neural language models. *ArXiv Preprint ArXiv:2001.08361*, 2020.
- Zichen Liu, Changyu Chen, Wenjun Li, Penghui Qi, Tianyu Pang, Chao Du, Wee Sun Lee, and Min Lin. Understanding rl-zero-like training: A critical perspective. *arXiv preprint arXiv:2503.20783*, 2025.
- Michael Noukhovitch, Shengyi Huang, Sophie Xhonneux, Arian Hosseini, Rishabh Agarwal, and Aaron Courville. Asynchronous rlhf: Faster and more efficient off-policy rl for language models. *arXiv preprint arXiv:2410.18252*, 2024.

- Long Ouyang, Jeffrey Wu, Xu Jiang, Diogo Almeida, Carroll Wainwright, Pamela Mishkin, Chong Zhang, Sandhini Agarwal, Katarina Slama, Alex Ray, et al. Training language models to follow instructions with human feedback. *Advances in neural information processing systems*, 35:27730–27744, 2022.
- John Schulman, Filip Wolski, Prafulla Dhariwal, Alec Radford, and Oleg Klimov. Proximal policy optimization algorithms. *ArXiv Preprint ArXiv:1707.06347*, 2017a.
- John Schulman, Filip Wolski, Prafulla Dhariwal, Alec Radford, and Oleg Klimov. Proximal policy optimization algorithms. *arXiv preprint arXiv:1707.06347*, 2017b.
- Zhihong Shao, Peiyi Wang, Qihao Zhu, Runxin Xu, Junxiao Song, Xiao Bi, Haowei Zhang, Mingchuan Zhang, YK Li, Yang Wu, et al. Deepseekmath: Pushing the limits of mathematical reasoning in open language models. *arXiv preprint arXiv:2402.03300*, 2024.
- Vaishnavi Shrivastava, Ahmed Awadallah, Vidhisha Balachandran, Shivam Garg, Harkirat Behl, and Dimitris Papailiopoulos. Sample more to think less: Group filtered policy optimization for concise reasoning. *arXiv preprint arXiv:2508.09726*, 2025.
- Prime Intellect Team, Sami Jaghouar, Justus Mattern, Jack Min Ong, Jannik Straube, Manveer Basra, Aaron Pazdera, Kushal Thaman, Matthew Di Ferrante, Felix Gabriel, et al. Intellect-2: A reasoning model trained through globally decentralized reinforcement learning. *arXiv preprint arXiv:2505.07291*, 2025.
- Garrett Warnell, Nicholas Waytowich, Vernon Lawhern, and Peter Stone. Deep tamer: Interactive agent shaping in high-dimensional state spaces. In *Proceedings of the AAAI conference on artificial intelligence*, pp. 1545–1553, 2018.
- Bo Wu, Sid Wang, Yunhao Tang, Jia Ding, Eryk Helenowski, Liang Tan, Tengyu Xu, Tushar Gowda, Zhengxing Chen, Chen Zhu, et al. Llamarl: A distributed asynchronous reinforcement learning framework for efficient large-scale llm trainin. *arXiv preprint arXiv:2505.24034*, 2025.
- Changyi Xiao, Mengdi Zhang, and Yixin Cao. Bnpo: Beta normalization policy optimization. *arXiv preprint arXiv:2506.02864*, 2025.
- An Yang, Anfeng Li, Baosong Yang, Beichen Zhang, Binyuan Hui, Bo Zheng, Bowen Yu, Chang Gao, Chengen Huang, Chenxu Lv, Chujie Zheng, Dayiheng Liu, Fan Zhou, Fei Huang, Feng Hu, Hao Ge, Haoran Wei, Huan Lin, Jialong Tang, Jian Yang, Jianhong Tu, Jianwei Zhang, Jianxin Yang, Jiayi Yang, Jing Zhou, Jingren Zhou, Junyang Lin, Kai Dang, Keqin Bao, Kexin Yang, Le Yu, Lianghao Deng, Mei Li, Mingfeng Xue, Mingze Li, Pei Zhang, Peng Wang, Qin Zhu, Rui Men, Ruize Gao, Shixuan Liu, Shuang Luo, Tianhao Li, Tianyi Tang, Wenbiao Yin, Xingzhang Ren, Xinyu Wang, Xinyu Zhang, Xuancheng Ren, Yang Fan, Yang Su, Yichang Zhang, Yinger Zhang, Yu Wan, Yuqiong Liu, Zekun Wang, Zeyu Cui, Zhenru Zhang, Zhipeng Zhou, and Zihan Qiu. Qwen3 technical report. *arXiv preprint arXiv:2505.09388*, 2025.
- Han Zhang, Yu Lei, Lin Gui, Min Yang, Yulan He, Hui Wang, and Ruifeng Xu. Cppo: Continual learning for reinforcement learning with human feedback. In *The Twelfth International Conference on Learning Representations*, 2024.
- Chujie Zheng, Shixuan Liu, Mingze Li, Xiong-Hui Chen, Bowen Yu, Chang Gao, Kai Dang, Yuqiong Liu, Rui Men, An Yang, et al. Group sequence policy optimization. *arXiv preprint arXiv:2507.18071*, 2025.
- Daniel M Ziegler, Nisan Stiennon, Jeffrey Wu, Tom B Brown, Alec Radford, Dario Amodei, Paul Christiano, and Geoffrey Irving. Fine-tuning language models from human preferences. *arXiv preprint arXiv:1909.08593*, 2019.

A THEORETICAL PROOF OF IMPORTANCE SAMPLING VARIANCE

This appendix analyzes a newly proposed importance sampling weight $w_{\text{new}}(x) = \frac{p(x)}{\mathbb{E}_q[q]}$, where $\mathbb{E}_q[q] = \int q(x)^2 dx$, and compares its variance with the standard importance sampling weight $w_{\text{std}}(x) = \frac{p(x)}{q(x)}$.

Problem Setting Let the target distribution be $p(x)$ and the proposal distribution be $q(x)$. We aim to estimate:

$$\mathbb{E}_p[f] = \int f(x)p(x)dx. \quad (6)$$

Since direct sampling from p is difficult, we employ importance sampling by drawing samples from q .

Standard Importance Sampling The standard weight is defined as:

$$w_{\text{std}}(x) = \frac{p(x)}{q(x)}. \quad (7)$$

Its expectation under q is:

$$\mathbb{E}_q \left[\frac{p(x)}{q(x)} \right] = \int \frac{p(x)}{q(x)} q(x) dx = \int p(x) dx = 1, \quad (8)$$

thus it is unbiased. Its variance is:

$$\begin{aligned} \text{Var}_q(w_{\text{std}}) &= \mathbb{E}_q \left[\left(\frac{p}{q} \right)^2 \right] - \left(\mathbb{E}_q \left[\frac{p}{q} \right] \right)^2 \\ &= \int \frac{p(x)^2}{q(x)} dx - 1. \end{aligned} \quad (9)$$

Denoted as:

$$\text{Var}_{\text{std}} = \int \frac{p(x)^2}{q(x)} dx - 1. \quad (10)$$

Group Expectation Importance Sampling The new weight is defined as:

$$w_{\text{new}}(x) = \frac{p(x)}{\mathbb{E}_q[q]}, \quad \text{where } \mathbb{E}_q[q] = \int q(x)^2 dx. \quad (11)$$

Its expectation is:

$$\mathbb{E}_q[w_{\text{new}}] = \frac{1}{\mathbb{E}_q[q]} \int p(x)q(x)dx = \frac{\langle p, q \rangle}{\|q\|_2^2}, \quad (12)$$

where $\langle p, q \rangle$ denotes the inner product $\int p(x)q(x)dx$. Generally, $\langle p, q \rangle \neq \|q\|_2^2$, making this estimator biased. Its variance is:

$$\begin{aligned} \text{Var}_q(w_{\text{new}}) &= \mathbb{E}_q \left[\left(\frac{p(x)}{\mathbb{E}_q[q]} \right)^2 \right] - \left(\mathbb{E}_q \left[\frac{p(x)}{\mathbb{E}_q[q]} \right] \right)^2 \\ &= \frac{1}{(\mathbb{E}_q[q])^2} \left(\int p(x)^2 q(x) dx - \left(\int p(x)q(x) dx \right)^2 \right). \end{aligned} \quad (13)$$

Denoted as:

$$\text{Var}_{\text{new}} = \frac{1}{(\int q(x)^2 dx)^2} \left(\int p(x)^2 q(x) dx - \left(\int p(x)q(x) dx \right)^2 \right). \quad (14)$$

Variance Comparison We compare:

$$\begin{aligned} \text{Var}_{\text{std}} &= \int \frac{p(x)^2}{q(x)} dx - 1, \\ \text{Var}_{\text{new}} &= \frac{1}{\left(\int q(x)^2 dx\right)^2} \left(\int p(x)^2 q(x) dx - \left(\int p(x) q(x) dx \right)^2 \right). \end{aligned} \quad (15)$$

A.1 VARIANCE COMPARISON IN DISCRETE SPACE

Since the action space of large models is discrete, this section discusses the variance difference $\Delta = \text{Var}_{\text{std}} - \text{Var}_{\text{new}}$ in discrete probability space. The integral expressions in the continuous case naturally transition to discrete summation forms:

- Replace continuous integrals $\int \cdot dx$ with discrete summations $\sum_{i=1}^n$;
- Replace probability density functions $p(x)$, $q(x)$ with probability masses p_i , q_i ;
- Maintain the structural form of variance expressions unchanged.

Notation and Setting Let the sample space be a finite set $\mathcal{X} = \{1, 2, \dots, n\}$, where $n \geq 2$. Let $p = (p_1, \dots, p_n)$ and $q = (q_1, \dots, q_n)$ be two probability distributions satisfying:

- $p_i > 0$, $\sum_{i=1}^n p_i = 1$,
- $q_i > 0$, $\sum_{i=1}^n q_i = 1$.

Define the following four key quantities, corresponding to the integral terms in the continuous expressions:

$$A = \left(\sum_{i=1}^n q_i^2 \right)^2, \quad (\text{corresponding to } \left(\int q(x)^2 dx \right)^2) \quad (16)$$

$$B = \left(\sum_{i=1}^n p_i q_i \right)^2, \quad (\text{corresponding to } \left(\int p(x) q(x) dx \right)^2) \quad (17)$$

$$I_1 = \sum_{i=1}^n \frac{p_i^2}{q_i}, \quad (\text{corresponding to } \int \frac{p(x)^2}{q(x)} dx) \quad (18)$$

$$I_2 = \sum_{i=1}^n p_i^2 q_i, \quad (\text{corresponding to } \int p(x)^2 q(x) dx) \quad (19)$$

Accordingly, the variance difference can be written as:

$$\Delta = I_1 + \frac{B - A - I_2}{A}. \quad (20)$$

Lemma 1 (Range of Quantities). *Under the above setting, we have:*

- $A \in \left[\frac{1}{n^2}, 1 \right]$,
- $B \in [0, 1]$,
- $I_1 \in [1, \infty)$,
- $I_2 \in (0, 1]$.

Proof.

1. **Range of A:** By the power mean inequality, $\sum q_i^2 \geq \frac{1}{n}$, and $\sum q_i^2 \leq 1$, thus $A \in [1/n^2, 1]$.
2. **Range of B:** $\sum p_i q_i \in (0, 1]$, thus $B \in [0, 1]$.
3. **Range of I_1 :** By the Cauchy-Schwarz inequality, $I_1 \geq 1$, and it can approach infinity.
4. **Range of I_2 :** Since $p_i^2 \leq p_i$, we have $I_2 \leq 1$, and $I_2 > 0$. \square

Theorem 1. Let p, q be discrete probability distributions. Then there exists a constant C such that:

$$\text{Var} \left[\frac{p(y|x)}{q(y|x)} \right] - \text{Var} \left[\frac{p(y|x)}{\widehat{\mathbb{E}}_q[q(y|x)]} \right] \geq \exp(D_{\text{KL}}(p||q)) - C. \quad (21)$$

In particular, when $D_{\text{KL}}(p||q) > \log C$, it holds that $\text{Var}[\frac{p(y|x)}{q(y|x)}] > \text{Var}[\frac{p(y|x)}{\widehat{\mathbb{E}}_q[q(y|x)]}]$.

Proof. Step 1. From the fundamental inequality relationship between KL divergence and χ^2 divergence (Pinsker's inequality):

$$D_{\text{KL}}(p||q) \leq \log(1 + D_{\chi^2}(p||q)), \quad (22)$$

where the chi-square divergence is defined as:

$$D_{\chi^2}(p||q) = \sum_{i=1}^n \frac{(p_i - q_i)^2}{q_i} = \sum_{i=1}^n \frac{p_i^2}{q_i} - 1 = I_1 - 1. \quad (23)$$

Substituting yields:

$$D_{\text{KL}}(p||q) \leq \log(I_1), \quad (24)$$

therefore:

$$I_1 \geq \exp(D_{\text{KL}}(p||q)). \quad (25)$$

Step 2. From Lemma 1, we know that A , B , and I_2 satisfy the following bounds:

$$A \in [\frac{1}{n^2}, 1], \quad (26)$$

$$B \in [0, 1], \quad (27)$$

$$I_2 \in (0, 1]. \quad (28)$$

Consider the lower bound of the expression $\frac{B - A - I_2}{A}$. To obtain its minimum value, we take:

- Minimum value of B : $B = 0$
- Minimum value of A : $A = \frac{1}{n^2}$
- Maximum value of I_2 : $I_2 = 1$

Substituting yields:

$$\frac{B - A - I_2}{A} \geq \frac{0 - 1/n^2 - 1}{1/n^2} = -(n^2 + 1). \quad (29)$$

Step 3. Substituting inequalities (1) and (2) into the expression for Δ :

$$\Delta = I_1 + \frac{B - A - I_2}{A} \geq \exp(D_{\text{KL}}(p||q)) - (n^2 + 1). \quad (30)$$

When $D_{\text{KL}}(p||q) > \log(n^2 + 1)$, we have:

$$\exp(D_{\text{KL}}(p||q)) > n^2 + 1, \quad (31)$$

thus:

$$\Delta > 0, \quad (32)$$

i.e., $\text{Var}_{\text{std}} > \text{Var}_{\text{new}}$. □

Corollary 1. In discrete space, if $D_{\text{KL}}(p||q) > \log(n^2 + 1)$, then:

$$\text{Var}_{\text{std}} > \text{Var}_{\text{new}}, \quad (33)$$

i.e., the new estimator has smaller variance.

It should be noted that A only attains the value $\frac{1}{n^2}$ when q follows a uniform distribution. In practice, when large models generate responses, the distribution tends to be long-tailed, so the value of A is much greater than $\frac{1}{n^2}$, and the constant $C_{\text{real}} \ll \log(n^2 + 1)$. For example, we randomly generated 128 tokens using Qwen3-1.7B ($n = 151936$), and the standard variance and average of A was $0.432 \pm 0.36 \gg \frac{1}{n^2}$.

B SUPPLEMENTARY EXPERIMENTS

B.1 IMPLEMENTATION DETAILS

All experiments use the Qwen3-1.7B model with a maximum input length of 768 and output length of 2048 tokens under both think and no-think mode, limited by computational constraints and low token efficiency (Shrivastava et al., 2025) (reward/length) at full context length. Training follows a GRPO-like algorithm with a learning rate of 1×10^{-6} , 3% linear warmup, per-device batch size 8, and gradient accumulation of 1, with gradient checkpointing enabled for memory efficiency. Evaluations occur every 32 or 64 steps. To model network latency in heterogeneous environments, we introduce a log-normal delay simulator bounded between 60 and 1800 seconds (99.5% CI), with default delay at 60 seconds and policy staleness varied across 0–64 effective steps. For online training, KL divergence is not used; for heterogeneous settings, CPPO-KL (Zhang et al., 2024) loss with coefficient 0.005 is applied. Rollouts are generated using vLLM with 8 parallel responses per prompt, and each run lasts 3 epochs, with metrics logged via Weights & Biases. The system prompt used in the experiments is shown in Figure 8.

[think mode] You are a helpful AI Assistant, designed to provided well-reasoned and detailed responses. You FIRST think about the reasoning process as an internal monologue and then provide the user with the answer. Please put your final answer within `\boxed{}`. Also, indicate that it is the answer.

[no-think mode] You are a helpful AI Assistant, designed to provided well-reasoned and detailed responses. Please put your final answer within `\boxed{}`. Also, indicate that it is the answer.

Figure 8: System prompt (thinking mode) of all trainings in our experiments.

B.2 COMPARISON OF THINK AND NON-THINK MODE

Under the non-thinking mode, all methods exhibit constrained exploration capacity, reflected in generally lower Last scores compared to their Best counterparts — indicating difficulty in maintaining performance stability during later training stages.

Notably:

- GEPO (ours) consistently achieves the highest Best and Last scores across all benchmarks and delay settings, demonstrating superior sample efficiency and convergence stability even without thinking steps.
- Under Max Tolerable Delay = 0, GEPO outperforms the strongest baseline (GSPO) by +3.7 points in average Best and a remarkable +20.8 points in average Last, highlighting its robustness against premature performance collapse.
- When Delay = 64 is allowed, most baselines show improved Last scores (e.g., Dr.GRPO improves from 0.0 to 33.4), suggesting that minimal computational slack helps stabilize training. GEPO again leads with the highest retention of peak performance (Last = 38.0 vs. 35.7 for GRPO).
- The vanilla Qwen3-1.7B model (non-RL baseline) achieves 33.2 average Best, which is surpassed by all RL methods — confirming the value of policy optimization even in non-think mode.

In summary, while non-think mode inherently limits reasoning depth, GEPO demonstrates exceptional training stability and final performance, making it the most reliable choice under strict latency or real-time constraints.

A systematic comparison between reinforcement learning under **think** and **non-think** modes reveals fundamental trade-offs between reasoning capacity, training stability, computational cost, and final performance. Key observations are summarized below:

Table 2: Performance comparison using Qwen3-1.7B (non-thinking mode).

Method	AMC23		AIME2024		AIME2025		MATH500		Average	
	Best	Last	Best	Last	Best	Last	Best	Last	Best	Last
Qwen3-1.7B	42.8	-	10.2	-	9.4	-	70.2	-	33.2	-
Max Tolerable Delay 0										
Dr.GRPO	45.0	0.0	14.4	0.0	11.3	0.0	73.6	0.0	36.1	0.0
GRPO	50.0	28.8	16.4	7.8	13.7	7.2	77.5	59.7	39.4	25.9
GSPO	53.1	23.8	14.4	2.7	16.0	0.4	76.5	55.6	40.0	20.6
GEPO (ours)	55.0	52.5	22.3	22.3	18.4	13.7	79.2	77.1	43.7	41.4
Max Tolerable Delay 64										
Dr.GRPO	45.0	41.6	14.1	9.7	13.3	10.1	72.5	72.3	36.2	33.4
GRPO	46.3	46.3	14.5	14.5	13.6	10.1	72.6	71.7	36.8	35.7
GSPO	47.2	36.6	13.7	4.3	13.3	8.9	75.1	67.9	37.3	29.4
GEPO (ours)	52.5	52.5	14.5	10.2	14.5	12.1	77.4	77.1	39.7	38.0

1) Performance Ceiling and Stability Under Max Tolerable Delay = 0, where no additional computation is allowed for reasoning:

- In **non-think** mode, GEPO achieves 43.7 average Best and 41.4 Last, demonstrating exceptional stability — the gap between Best and Last is minimal.
- In **think** mode, the same method (GEPO) reaches 44.9 Best and 41.4 Last, showing only a marginal gain in peak performance (+1.2) but identical final performance.
- Notably, baselines like GRPO and GSPO in **think** mode exhibit larger Best–Last gaps (e.g., GRPO: 44.2 → 19.0), indicating that thinking can destabilize training if not properly regularized.

2) Impact of Delay Tolerance When Delay = 64 is permitted:

- In **non-think** mode, most methods show dramatic Last score improvements (e.g., Dr.GRPO: 0.0 → 33.4; GRPO: 25.9 → 35.7), suggesting that even minimal training-time slack mitigates collapse.
- In **think** mode, GEPO achieves perfect retention (Last = Best = 43.5), while others still suffer degradation (e.g., GSPO: 41.9 → 20.9). This confirms that **thinking introduces optimization instability unless explicitly controlled**.

3) Role of Thinking in Exploration vs. Efficiency As shown in Figure 9:

- **Think** mode consistently produces longer rollouts (Avg. and Terminated Length), indicating deeper exploration and more deliberate reasoning.
- However, it also leads to significantly higher overlength ratios, especially early in training — implying wasted computation and potential divergence risk.
- In contrast, **non-think** mode yields shorter, more efficient rollouts with lower overlength risk, yet still achieves competitive or even superior final performance when paired with stable algorithms like GEPO.

While **think** mode enables deeper reasoning and occasionally higher peak scores, it introduces training instability and computational overhead. **Non-think** mode, especially when combined with robust policy optimization (e.g., GEPO), offers a more **stable, efficient, and often equally effective** alternative — particularly under real-time or latency-constrained deployment scenarios. The choice between modes should be guided by the application’s tolerance for delay, need for interpretability, and performance stability requirements.

Figure 9 compares the rollout lengths under **think** and **non-think** modes during GEPO training. The figure consists of three subplots analyzing rollout length characteristics from different perspectives:

- **(a) Average Length** shows the trend of average rollout steps versus training steps. The red curve (GEPO with **think**) consistently lies above the blue curve (GEPO without **think**), indicating that the agent generates longer sequences under **think** mode, possibly due to additional reasoning steps or policy adjustments.
- **(b) Terminated Length** represents the length of rollouts that successfully terminate. Again, **think** mode yields significantly longer terminated rollouts, suggesting that the thinking mechanism enables the agent to explore longer, valid trajectories.
- **(c) Overlength Ratio** reflects the proportion of rollouts exceeding a predefined length threshold. The **think** mode exhibits a notably higher overlength ratio, especially in early training stages, indicating that while **think** enhances exploration, it may also lead to unnecessarily long rollouts, increasing computational cost.

Comprehensive Analysis: These results reveal the impact of **think** mode on rollout behavior — it extends effective exploration paths and improves task completion quality, but also introduces a higher risk of overlength rollouts. In practice, one must balance the benefits of ‘thinking’ against potential efficiency losses, possibly by imposing length constraints or employing dynamic adjustment mechanisms to optimize performance.

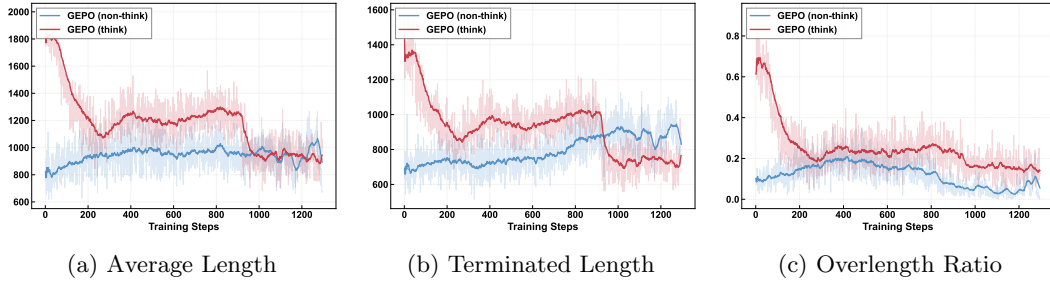


Figure 9: Comparison of rollout (clipped by 2k tokens) lengths under think and non-think modes.

C NETWORK LATENCY

We test the performance limits of GEPO and baseline methods in simulated network delay scenarios and train the model on heterogeneous computing resources connected through a real-world internet connection.

C.1 SIMULATED NETWORK LATENCY CONFIGURATION

Our goal is to simulate RL training of large models over internet-connected heterogeneous compute clusters, where network delays are inherently uncertain. To evaluate algorithmic performance and training stability under extreme and variable latency conditions, we employ three widely used delay distributions P_d : log-normal, Weibull, and exponential. We set a high maximum delay threshold of 1800 seconds, which is sufficient to cover typical model and data transmission times. In our simulation, model parameter synchronization and rollout data transfer are implemented as follows:

- **Learner saves model:** The learner periodically saves model checkpoints to a shared model file path `Model_Sync_Path` via `torch.save_pretrained()`.
- **Sampler loads model:** The sampler generates data using the current model until a delay D_M , drawn from P_d , elapses. It then loads the latest model from `Model_Sync_Path`. The sampler remains active throughout—no idling occurs.

- **Sampler sends data:** Generated rollout batches are saved to `Rollout.Sync.Path` with timestamp T_{sync} . To simplify implementation, data transmission is assumed instantaneous; its latency is effectively merged into the model sync delay D_M , without affecting simulation validity.
- **Learner uses data:** The learner trains on rollout data from `Rollout.Sync.Path` that falls within a recent time window (e.g., no older than 1800 seconds).

C.2 REAL-WORLD NETWORK SCENARIOS

To evaluate the performance of heterogeneous reinforcement learning algorithms in realistic network environments, we develop a communication toolkit based on ZeroMQ, supporting TCP/IP-based transmission of inference trajectories from samplers to learners and synchronized model parameter updates. As shown in Figure 10, the toolkit enables multi-node communication over wide-area networks (WANs), with the following core communication logic:

- The learner continuously listens for and buffers inference trajectory messages from samplers. It automatically updates its trajectory buffer upon message arrival and broadcasts the latest model parameters to all connected samplers once a predefined synchronization interval is reached.
- After generating an inference trajectory, the sampler sends it to the learner and continuously listens for parameter update messages. Upon receiving new model parameters, the sampler updates its local parameters and resumes sampling before the next sampling step.

Key features of the communication toolkit include:

1) Many-to-Many Communication Pattern The toolkit supports elastic node scaling with dynamically reconfigurable routing topologies, enabling seamless adaptation to node join/leave events. This facilitates efficient distributed parameter synchronization and trajectory collection in large-scale deployments.

2) Chunked Message Transmission Inspired by Shardcast, the toolkit employs adaptive message chunking for both model parameters and trajectory data. The chunk size is dynamically adjusted according to real-time bandwidth conditions. At the receiver side, chunks are reassembled and integrity-verified, effectively mitigating the impact of high latency in wide-area networks.

3) Communication Safety Mechanisms Thread-safe message passing across multiple processes is ensured via a double-buffering queue design and fine-grained locking. This prevents race conditions during concurrent read/write operations and guarantees reliable parameter synchronization.

4) Configurable Routing Topology The toolkit supports user-defined connectivity patterns between learners and samplers, accommodating asymmetric node configurations (e.g., one learner connected to four samplers). This enhances communication flexibility and scalability in dynamic, heterogeneous environments.

D FROM TOKEN-LEVEL TO GROUP-LEVEL IMPORTANCE WEIGHT

D.1 TOKEN-LEVEL IMPORTANCE WEIGHT

In traditional policy optimization methods, such as GRPO (Shao et al., 2024) or PPO (Schulman et al., 2017a), importance sampling is typically performed at the `token-level`. Specifically, for a generated sequence $y = (y_1, \dots, y_T)$, the importance weight is computed token by token:

$$w_{token} = \text{clip} \left(\frac{p(y_t | x, y_{<t})}{q(y_t | x, y_{<t})}, 1 - \epsilon, 1 + \epsilon \right), \quad (34)$$

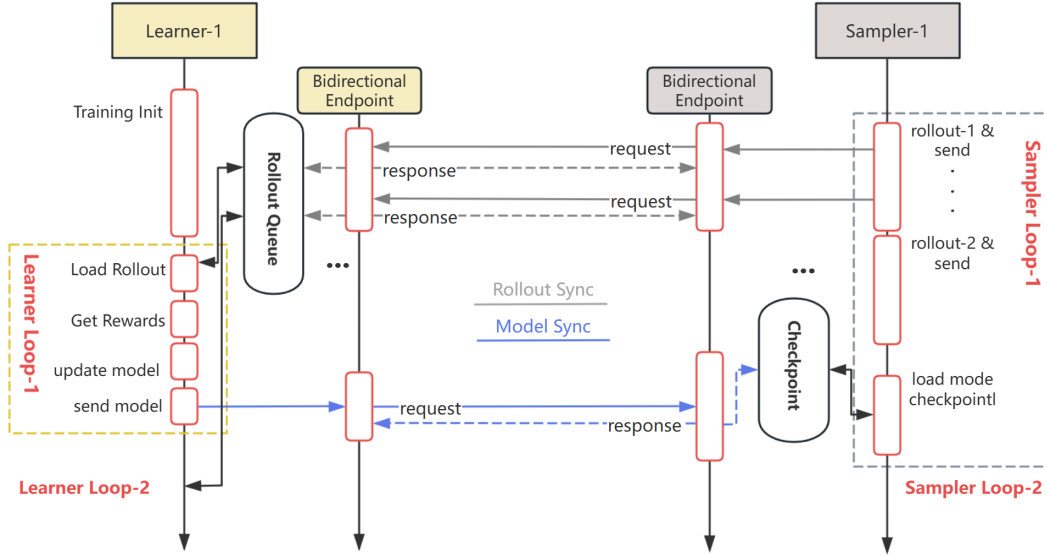


Figure 10: Communication flow between a learner and sampler in a distributed reinforcement learning system, showing trajectory collection and model synchronization over a bidirectional endpoint.

and used to compute the policy gradient at each time step. However, this per-token reweighting scheme suffers from two key limitations:

1) Inconsistency between optimization and reward granularity: Concurrent work such as GSPO (Zheng et al., 2025) argues that since the reward is assigned at the sequence level—i.e., to the full response y —the importance weighting for policy updates should also operate at the same granularity, rather than at the token level.

2) High variance in token-level probabilities: Beyond this alignment issue, we provide an explanation from the perspective of importance weight variance: because the final reward depends on the entire sample, large local changes in token probabilities can lead to extreme values in the ratio $\frac{p(y_t|x, y_{<t})}{q(y_t|x, y_{<t})}$. This inflates the variance of token-level importance weights, causing them to frequently fall outside the clipping range. Once clipped, gradients for these tokens are effectively zeroed out due to the stop-gradient behavior of `torch.clamp`, preventing meaningful updates. As a result, tokens that require large corrections may be ignored, leading to inefficient optimization.

D.2 SAMPLE-LEVEL IMPORTANCE WEIGHT

The **sample-level** importance weighting treats the entire response as a sampling unit and computing the weight based on its full conditional probability. Given a prompt x , both the target policy $p(y|x)$ and the behavior policy $q(y|x)$ are defined as the joint probability of the sequence:

$$p(y|x) = \left| \prod_{t=1}^T p(y_t | x, y_{<t}) \right|^{\frac{1}{T}}, \quad q(y|x) = \left| \prod_{t=1}^T q(y_t | x, y_{<t}) \right|^{\frac{1}{T}}. \quad (35)$$

The sample-level importance weight is then:

$$w_{\text{sequence}}(y|x) = \text{clip} \left(\frac{p(y|x)}{q(y|x)}, 1 - \epsilon, 1 + \epsilon \right). \quad (36)$$

This formulation computes the full sequence-level ratio before clipping, thereby avoiding premature truncation caused by high-variance individual tokens. By preserving gradient flow across the entire sequence, sample-level weighting enables more stable and effective policy updates, especially under high policy divergence induced by network latency.

D.3 GROUP-LEVEL IMPORTANCE WEIGHT

Group-level importance weighting represents a paradigm shift in reinforcement learning optimization by recognizing that policy updates should not only align with the granularity of reward assignment but also leverage higher-order statistical relationships among multiple samples. The key insight is that individual samples should not be treated in isolation; instead, their collective behavior under the same prompt provides crucial information for stable policy updates. By considering the expected value of proposal probabilities within a group of responses, we effectively smooth out the erratic fluctuations that plague token-level and even sequence-level weighting schemes. This approach acknowledges an important reality of distributed training: in heterogeneous environments with network latency, policy divergence is inevitable, and our optimization methods must be designed to gracefully handle—not merely tolerate—this divergence. The group-level perspective transforms what was previously seen as a limitation (policy staleness due to latency) into an opportunity for more robust learning through statistical regularization of importance weights.

E DEFENSIVE SAMPLING AND SMOOTH DENOMINATOR MECHANISM

To mitigate potential bias introduced by replacing the denominator and further enhance robustness, we introduce a defensive sampling mechanism that incorporates the target policy probability into the denominator:

$$w_{\text{final}}(y|x) = \frac{p(y|x)}{\epsilon \cdot p(y|x).\text{detach}() + (1 - \epsilon) \cdot \widehat{\mathbb{E}}_q[q(y|x)]}, \quad (37)$$

where $\epsilon \propto \text{Var}(q) \in (0, 1)$ is a smoothing coefficient, and $p(y|x).\text{detach}()$ denotes stopping gradient propagation during backpropagation. We employ a heuristic strategy that sets ϵ proportional to the variance of q , which we find in most experimental settings leads to improved training stability. A higher $\text{Var}(q)$ indicates greater bias from using the GEIS approximation (i.e., larger $(q - \widehat{\mathbb{E}}_q[q(y|x)])^2$), so increasing ϵ reduces reliance on the potentially biased $\widehat{\mathbb{E}}_q[q(y|x)]$ and shifts the objective toward the policy gradient update.

Notably, the standard policy gradient objective $\log p(y|x) \cdot A(x, y)$ produces gradients of the form $\frac{p'_\theta(y|x) \cdot A(x, y)}{p(y|x).\text{detach}()}$, which is equivalent to the gradient induced by $w_{\text{final}}(y|x) \cdot A(x, y)$ when $\epsilon = 1$. Since policy gradients do not rely on importance sampling, they are inherently immune to high variance in importance weights under large network delays. This design exhibits the following properties:

- When $p(y|x)$ is high, the denominator adapts locally, preserving the weight magnitude for high-probability samples;
- When $\text{Var}(q)$ is low, the denominator reverts to the group average, avoiding numerical instability;
- When $\text{Var}(q)$ is high, the objective smoothly transitions toward the policy gradient update, avoiding the detrimental effects of high-variance importance weights;
- The overall weighting scheme produces smoother weight distributions and reduced gradient variance, leading to more stable and efficient training under asynchronous, heterogeneous conditions.

F THE COMPARISON OF DIFFERENT REINFORCEMENT LEARNING PARADIGMS

F.1 CORE CHALLENGE: OFF-POLICY LEARNING AND IMPORTANCE SAMPLING

This formulation highlights the central challenge in asynchronous RL: the mismatch between the behavior policy (π_{θ_k}) and the target policy ($\pi_{\theta_{k+\tau}}$), which grows with τ and introduces

bias and variance into the learning process. Addressing this mismatch under high and uncertain latency is the primary focus of our work.

The HeteroRL framework decouples rollout sampling from parameter learning, leading to a setting where the learner updates the new policy $\pi_{\theta_{k+\tau}}$ using data generated by an older policy π_{θ_k} —a canonical off-policy learning scenario. To correct for the distributional shift between the behavior and target policies, importance sampling (IS) is commonly employed. Under the GRPO framework, this weight is used to scale the advantage during policy gradient updates. However, when the delay τ is large, causing significant divergence between the policies (i.e., high KL divergence $D_{\text{KL}}(\pi_{\theta_{k+\tau}} \parallel \pi_{\theta_k})$), we observe in practice that the variance of the importance weights increases rapidly with τ , and the estimation error of the expected reward also grows. As a result, the variance of w_{std} explodes, introducing high noise into gradient estimates and ultimately leading to training instability or collapse. The central challenge of this work is thus to design a robust algorithm that mitigates the training instability caused by the explosion of importance sampling variance under high network latency.

Table 3: Core Characteristics of Online, Offline, and Heterogeneous Reinforcement Learning Paradigms

Aspect	Online RL	Offline RL	Heterogeneous RL
Data Generation	Online interaction: Data generated instantly by the current policy .	Fixed, pre-collected dataset: Uses static data collected by some (unknown) behavior policy.	Delayed interaction: Data generated by historical policy versions (due to unpredictable network delay).
Policy Version during Data Generation	Always current: Requires strict synchronization with the learning policy.	Fixed: The behavior policy is fixed and inherent to the dataset.	Dynamically stale: Staleness determined by unpredictable network delay (<i>core characteristic</i>).
System Architecture	Tightly-coupled: Actor (environment interaction) and Learner (parameter update) typically co-located or on a low-latency network.	Single-machine or simple distributed: No real-time interaction required; training is data-driven.	Geographically decoupled: Actor and Learner separated by a high-latency network , tolerant to delays.
Handling of System Latency	Treated as failure: Requires synchronization; latency causes resource idling and training stalls.	Not applicable: Training process has no real-time interaction .	Algorithmic compensation: Employs corrective techniques (e.g., importance sampling) to mitigate latency effects.
Core Challenge	Exploration-exploitation trade-off during learning. *Resource utilization* under sequential tasks.	Distributional shift and limited data coverage .	Algorithmic stability under dynamic delays: High/variable latency causes importance weight variance explosion .